

## Carboxymethyl Chitosan modified Montmorillonite for Efficient Removal of Cationic Dye from Waste Water

Pritha Mitra, Kishor Sarkar, and P.P. Kundu\*

*Department of Polymer Science and Technology, 92 APC Road, University of Calcutta, Kolkata-700 009, India*

*\*E-Mail: ppk923@yahoo.com*

### ABSTRACT

The feasibility of carboxymethyl chitosan intercalated montmorillonite (CMCTS-MMT) clay used as a low-cost and effective adsorbent for removal of cationic dye, crystal violet from the aqueous solution has been investigated. The synthesis of CMCTS-MMT was confirmed from the analytical information based on the characterization carried out by Fourier transformation infrared spectroscopy, x-ray diffraction data. During the removal process, batch technique was used and the effect of initial dye concentration, pH, temperature and weight ratio variation of sample composition were evaluated. Sorption process was analysed using pseudo-first order and pseudo-second order kinetic models. The data showed that the second order kinetic model was more appropriate for the absorption of the present dye. The equilibrium adsorption isotherms have been analyzed with the help of Langmuir, Freundlich and Redlich-Peterson analytical models. It was observed that the experimental data correlated reasonably well by the Redlich-Peterson and Langmuir isotherms. The desorbed CMCTS-MMT could be reused for adsorption of cationic dye. To investigate the changes in surface morphology of CMCTS-MMT after sorption, scanning electron microscopy analysis were done before and after adsorption of the cationic dye. Finally, the results in this study confirmed that CMCTS-MMT may be an attractive contender for removal of cationic dyes from the waste water.

**Keywords:** adsorption, basic dye, montmorillonite, kinetics, equilibrium isotherms

### 1. INTRODUCTION

Organic dyes are one of the most hazardous pollutants which are generally present in the effluents of textile, paper, leather, food, plastics, cosmetics and dye manufacturing industries<sup>1,2</sup>. Because of their synthetic origin and complex aromatic structure, it is really challenging task to treat the dye effluents as they are mostly biologically non-degradable and stable to light, heat<sup>3</sup>. Several treatment processes are known for the removal of dyes from wastewater, for example the processes of coagulation and flocculation<sup>4</sup>, oxidation<sup>5</sup>, membrane separation<sup>6</sup>, electro-coagulation<sup>7</sup>, integrated chemical-biological degradation<sup>8</sup>, solar photo-Fenton and biological processes<sup>9</sup> and adsorption on activated carbon, manganese, silica gel and clays<sup>10</sup>. Among these methods, adsorption on activated carbon is the most extensively used commercial practice due to the excellent adsorption capacity<sup>11</sup>. But due to the high cost and difficulty in the regeneration of activated carbon, new researches are encouraged for the development of effective adsorbents at a lower cost<sup>12</sup>. So far, a lot of low cost adsorbents have been tried such as to name a few orange peel<sup>13</sup>, waste metal hydroxide sludge<sup>14</sup>, broad bean peels<sup>15</sup>, rice husk<sup>16</sup>, palm kernel fibre<sup>17</sup>, fly ash<sup>18</sup>, pineapple stem<sup>19</sup>, acid-activated red mud<sup>20</sup> and others. But their adsorption performances are not quite impressive enough.

Recently, clay materials have attained much attraction as low cost and efficient adsorbents for dye removal treatment. Among the various kinds of clay materials, montmorillonite (MMT) has often been used for the removal of organic dye and

pigments due to their small particle size, lamellar structure and negatively charged surface. The chemical structure of MMT comprises a sheet like structure consisting of two tetrahedral silicate layers on either side and octahedral alumina layer in the middle. Na<sup>+</sup>-MMT belongs to the dioctahedral smectite group and consists of silicate layers that are separated by van der Waals' galleries. The surface of each silicate layer contains negatively electrical charges. When MMT is dispersed in water, it swells as a result of cation accumulation in the interlayer causing to increase its basal spacing. Although clays themselves possess high adsorption capabilities, the modification of their structure can successfully improve their proficiencies<sup>21</sup>.

Natural polymeric materials are another kind of important adsorbents as they are renewable, biodegradable, non-toxic and eco-friendly material. Chitosan based biosorbents have high affinity for various dyes and have wide range of applications in the biomedical, cosmetic, food and textile industries<sup>22</sup>. Because of its cationic nature, chitosan can absorb the cationic dyes in very small amounts. So, some chemical modifications of chitosan are necessary to improve their cationic dye adsorption properties. Carboxymethylation<sup>23,24</sup> of chitosan is a very smart method as it introduces active carboxyl (–COOH) groups into the molecule what makes it anionic in nature and facilitate cationic dyes adsorption<sup>25</sup>. But its solubility in water makes it difficult to reuse and the market cost is also relatively high. To overcome these problems some modifications are necessary. According to previous reports, chitosan could intercalate into layers of MMT under acidic conditions to modify and enhance

their adsorption capacity<sup>26,27</sup>. On further experimenting, we are quite sure that chitosan and its derivatives and clay have good potential for removal of dyes. However, still there is a need to find out the practical effectiveness of such developed adsorbents on commercial scale. Hence, we have prepared CMC intercalated MMT super adsorbent to improve the adsorption capacity for the removal of cationic dye crystal violet (CV) from aqueous solutions. CV (basic violet 3) is a very well-known dye which is extensively used in textile dyeing and paper printing purpose<sup>28</sup>.

The aim of the present study was to evaluate the viability of CMCTS-MMT as an economic and effective adsorbent for the removal of cationic dye CV in details. In this work, the effects of initial dye concentration, pH of the dye solution, adsorption temperature, adsorption time and weight ratio variation of composition on the adsorption process were studied. The sorption capacity of CMCTS-MMT was analysed using Langmuir, Freundlich and Redlich-Peterson isotherm models and the adsorption dynamics were scrutinized using pseudo first order and pseudo second order kinetic models. To explore its regeneration capacity the desorption study has also been carried out.

## 2. MATERIALS AND METHODS

### 2.1 Chemicals

The degree of deacetylation and weight average molecular weight,  $M_w$  (determined by GPC, gel permeation chromatography, Waters, USA) of chitosan (CTS) supplied by Acros Organics (USA) are 86 per cent and 222 kDa respectively. Monochloroacetic acid was obtained from Loba Chemie (India). Montmorillonite, a silicate clay (Sigma, USA) was used. All aqueous solutions were prepared in double distilled water. Other reagents used were all analytical grade and used without further purification.

### 2.2 Preparation of Crystal Violet Stock Solution

Crystal violet is a water soluble basic dye having the molecular formula  $C_{25}H_{30}ClN_3$  and CV used in this study was supplied by RFCL Ltd, India. The molecular weight of CV is 407.98 gm.mol<sup>-1</sup> and has  $\lambda_{max} = 588$  nm. Crystal violet stock solution of 4000 mg/L was prepared by dissolving 4 g of the dye into 1000 ml double distilled water. The pH of the dye solution was adjusted by adding dilute HCl or NaOH. The stock solution was used by fresh dilution during the entire experimental work.

### 2.3 Preparation of Carboxymethyl Chitosan

Carboxymethyl chitosan (CMCTS) was prepared according to the previous report<sup>29</sup> with slight modification. Briefly, 2 g of CTS was swelled in 40 ml isopropanol and water mixture (8:2 v/v ratio) containing 6 g NaOH at 50 °C for 1 hr. Then, monochloroacetic acid dissolved in isopropanol (3:4 v/v ratio) was added drop wise into the reaction mixture for 30 min. The reaction was continued with constant stirring for another 4 hr at the same temperature. Finally, the reaction was stopped by adding 70 per cent ethyl alcohol. The product was filtered and washed with 80 per cent ethyl alcohol to remove salt and water. The CMCTS was dried under vacuum overnight.

### 2.4 Preparation of CMCTS Intercalated MMT Adsorbent

Some modifications were done to the previous report<sup>30</sup> in the preparation of CMCTS intercalated MMT. 2.0 gm of MMT was dispersed in 50 ml of distilled water. Carboxymethyl chitosan solution was prepared by dissolving 0.5 gm of CMCTS in a 1 per cent (v/v) acetic acid aqueous solution and then pH was adjusted to 2.0 using a 20 wt per cent NaOH aqueous solution. The carboxymethyl chitosan solution was slowly added to MMT suspension followed by stirring at 60 °C for 6 h to obtain the carboxymethyl chitosan intercalated MMT (CMCTS-MMT). The products were washed with distilled water until the supernatant reached pH 7 and then dried at 60 °C for 12 h. The synthetic route of the sample is schematically shown in Fig. 1.

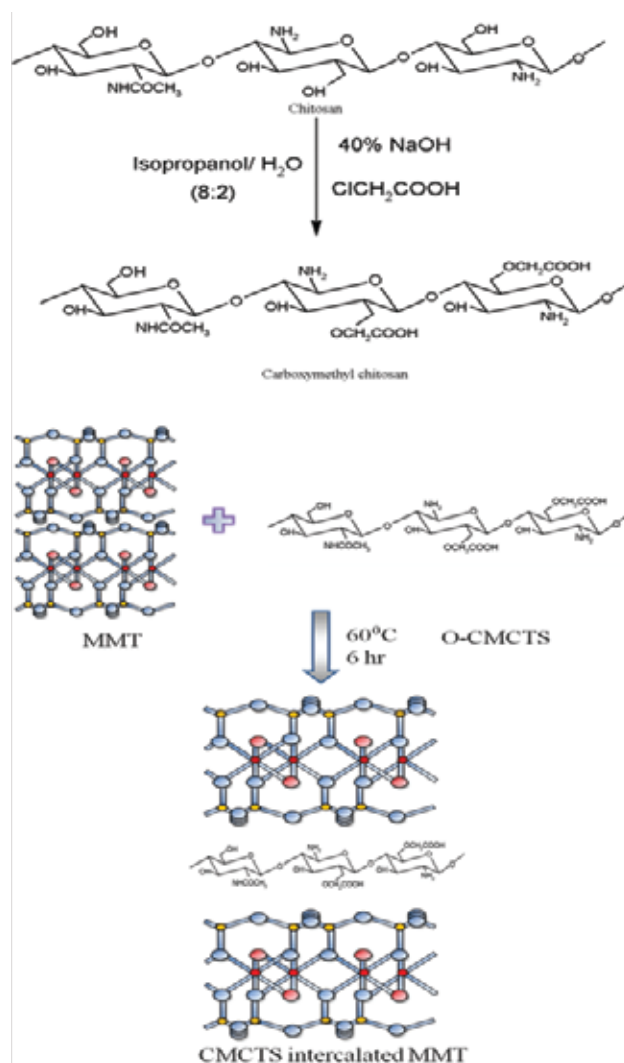


Figure 1. Synthesis route of CMCTS intercalated MMT adsorbent.

### 2.5 Characterization of CMCTS and CMCTS-MMT

#### 2.5.1 Infrared Spectroscopic Analysis

The samples were mixed with KBr powder to prepare pellets for infrared spectroscopic analysis (FTIR) analysis. The infrared spectra were recorded at the frequency range of 4000-500 cm<sup>-1</sup> with 42 consecutive scans at a 4 cm<sup>-1</sup> resolution on a Bruker Alpha ATR FTIR spectrometer. FTIR were carried out for CMCTS-MMT after adsorption to find their changes

in characteristics. The infrared spectral analysis was done to determine the functional groups responsible for the adsorption of dyes.

### 2.5.2 X-ray Diffraction (XRD) Analysis

X-ray diffraction spectroscopy of chitosan, CMCTS, MMT clay and CMCTS-MMT in the powder form were performed by a wide angle x-ray scattering diffractometer (Panalytical x-ray diffractometer, model- X'pert Pro) with Cu K $\alpha$  radiation ( $\lambda=1.5444$ ) in the range 5–50° (2 $\theta$ ) at 40 kV and 30 mA.

### 2.5.3 Scanning Electron Microscopy (SEM)

Scanning electron microscopy (SEM) analysis was carried out for CMCTS-MMT before and after dye adsorption to study their changes in the surface textures. About 10  $\mu$ L of complex suspension was deposited onto a glass slide and dried in room temperature. Before the SEM observation, the samples were fixed on an aluminum stub and coated with gold by ion sputter coater (Quoram, UK, Model-Q150T ES) for 7 min. The morphology of the sample was observed under a scanning electron microscope (ZEISS, EVO 18 special edition) at 10000x magnification and 15 kV.

## 2.6 Adsorption Studies by Batch Technique

Adsorption experiments were carried out by batch technique in a water bath and stirring with a magnetic stirrer at 200 rpm. In each study, 50 mg of CMCTS-MMT was added to 25 ml of an aqueous solution of CV at known concentrations in a 250 ml conical flask. The effects of initial dye concentration on the adsorption were carried out at 30 °C (pH 8) for 2 hours. The influence of pH on CV removal was studied by adjusting CV solutions (1600 mg/L) to different pH values (2, 4, 6, 8 and 10) at 30 °C for 2 hr. The effect of temperature on dye adsorption was carried out at different temperatures (25 °C, 30 °C, 40 °C, 50 °C and 60 °C) in 25 mL of dye solution (1600 mg/L, pH 8) with 0.05 g of CMCTS-MMT for 2 hr. For kinetic study, 1600 mg/L dye solutions (25 ml, pH 8) were agitated with 50 mg of adsorbent at 30 °C for 2 hr. Batch equilibrium adsorption experiments were carried out by agitating 25 ml of various dye concentrations of CV solution at pH 8.0 with 50 mg of adsorbent at 30 °C until equilibrium was established.

For kinetic study, the fixed amount of samples (50  $\mu$ l) was withdrawn from the flask at specific time intervals. The absorbencies of the samples were measured by using a uv-vis spectrophotometer at 588 nm. The amount of adsorption,  $Q$  (mg/g) was determined by the following equation.

$$Q = \frac{(C_0 - C_t)V}{W} \quad (1)$$

where  $C_0$  and  $C_t$  (mg/L) are the concentrations of dye initially and at time  $t$ , respectively.  $V$  is the volume of dye solution (L) and  $W$  is the mass (g) of dry adsorbent used.

## 2.7 Desorption Studies

Desorption studies help explain the nature of adsorption and recycling of the spent adsorbent and the dyes. With some modification of our previous report<sup>25</sup>, 50 mg of CMCTS-MMT

was loaded with 25 ml of 1600 mg/L CV solution at pH 8 for 180 min and agitation rate was maintained at 200 rpm. CV loaded CMCTS-MMT was separated from the dye solution by centrifugation. Then, the adsorbent was washed with distilled water to remove any unadsorbed dye. The amount of CV adsorbed per gram of the sample was obtained by analyzing the supernatant of CV solution. The loaded sample was agitated with 25 ml 0.2M HCl solution (pH 2) at 30 °C for 2 h and the sample was collected at different time intervals to determine the eluted dye concentration to calculate the percentage of desorption.

## 3. RESULT AND DISCUSSION

### 3.1 FT-IR Analysis

The FT-IR spectra of CTS, CMCTS, MMT, and CMCTS-MMT are shown in Fig. 2. Fig. 2(a) shows the basic characteristic peaks of CTS at 3428  $\text{cm}^{-1}$  (O-H stretch and N-H stretch, overlap), 2922  $\text{cm}^{-1}$  and 2860  $\text{cm}^{-1}$  (C-H stretch), 1653  $\text{cm}^{-1}$  (NH-CO (I) stretch), 1598  $\text{cm}^{-1}$  (N-H bend), 1381  $\text{cm}^{-1}$  (amide III), 1154  $\text{cm}^{-1}$  (bridge-O- stretch) and 1093  $\text{cm}^{-1}$  (C-O stretch). It is observed that the absorption band at 3382  $\text{cm}^{-1}$ , corresponding to the stretching vibrations of O-H and N-H groups of CTS is widened and weakened after carboxymethylation. The stretching vibration of NH-CO(I) group (1653  $\text{cm}^{-1}$ ), the bending vibration of N-H group (1598  $\text{cm}^{-1}$ ) and stretching vibration of the O-H group (1032  $\text{cm}^{-1}$ ) of CTS disappeared. In addition, the characteristic peak at 1601  $\text{cm}^{-1}$  due to the asymmetric stretching vibrations of carboxylate ( $-\text{COO}^-$ ) ions and N-H bending vibrations whereas the symmetric stretching vibration of carboxylate ( $-\text{COO}^-$ ) ions is observed at 1417  $\text{cm}^{-1}$  in the spectrum of CMCTS. So, the FTIR spectra indicate that carboxymethylation has occurred on both the amino and hydroxyl groups of CTS. In the IR studies of MMT clay, the Si-O and Si-O-Al stretching vibrations were observed at 791  $\text{cm}^{-1}$  and 674  $\text{cm}^{-1}$ , respectively, showing the presence of tetrahedral structure of Si and octahedral structure of Al. A strong band at 3626  $\text{cm}^{-1}$  as well as 3382.9  $\text{cm}^{-1}$  indicates the possible presence of the hydroxyl linkage (Al-O-H, inter octahedral). However, a broad band at 3383

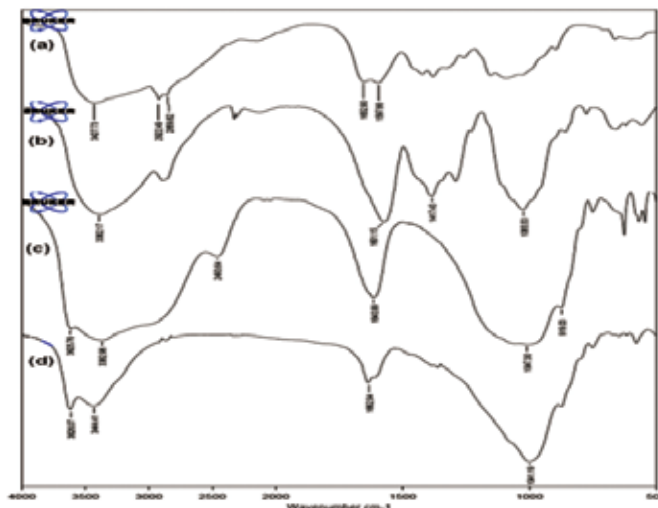


Figure 2. Infrared spectra of (a) CTS (b) CMCTS (c) MMT (d) CMCTS-MMT.

$\text{cm}^{-1}$  and a band at  $1644 \text{ cm}^{-1}$  in the spectrum of clay suggest the possible presence of water of hydration in the adsorbent.

Figure 2(d) shows the FTIR spectrum of CMCTS-MMT adsorbent. In intercalation process, no covalent bond was formed between CMCTS and MMT clay, only ionic interaction occurred. Therefore, no new absorption peak appeared in the FTIR spectrum of CMCTS-MMT.

### 3.2 XRD Analysis

CTS, CMCTS, MMT and CMCTS-MMT were put to the test XRD data and the patterns shown in Fig. 3. CTS showed two distinct crystalline peaks at around  $10^\circ$  and  $20^\circ$  due to 020 and 110 reflections, respectively. The presence of plenty of hydroxyl and amino groups in the CTS structure can help formation of stronger intermolecular and intra-molecular hydrogen bonds, leading to generation of regular crystalline structure in the CTS molecules. However, in case of CMCTS, the peak at  $10^\circ$  disappeared and the peak at  $20^\circ$  weakened. This may be attributed to the destruction of the intermolecular hydrogen bonds and the crystalline regions of CTS, indicating successful modification of chitosan. The peak at  $2\theta \approx 5.8^\circ$  was observed for pure MMT, corresponding to the periodicity in the direction perpendicular to the (001) plane of the clay. But, the peak intensity at  $2\theta \approx 5.8^\circ$  for CMCTS-MMT decreased after intercalation.

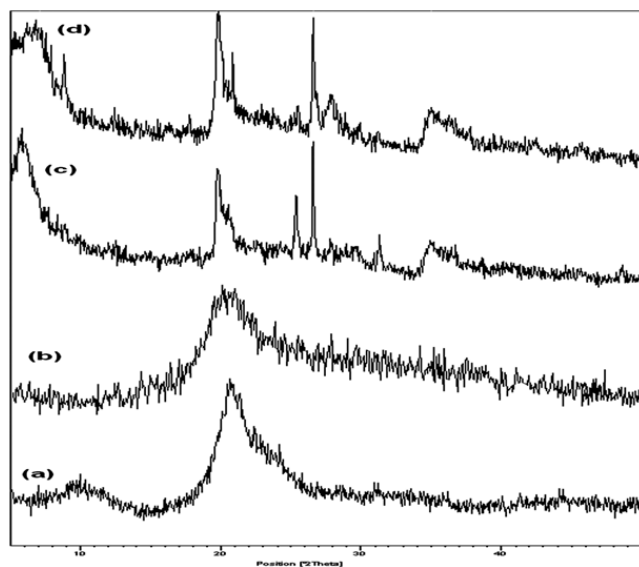


Figure 3. X-ray diffraction of (a) CTS (b) CMCTS (c) MMT (d) CMCTS-MMT.

### 3.3 SEM Analysis

The SEM micrograph of the CMCTS-MMT, before and after adsorption of the dye is presented in the Fig. 4. On analyzing the SEM images, one can observe the presence of highly heterogeneous pores within the sample before adsorption while the pores were observed to be packed with dyes after adsorption.

### 3.4 Adsorption Capacity of MMT, CTS-MMT and CMCTS-MMT

The adsorption capacity of MMT, CTS-MMT and CMCTS-MMT for CV at an initial concentration of  $400 \text{ mg/L}$  is shown in Fig. 5. It is observed that the adsorption capacity

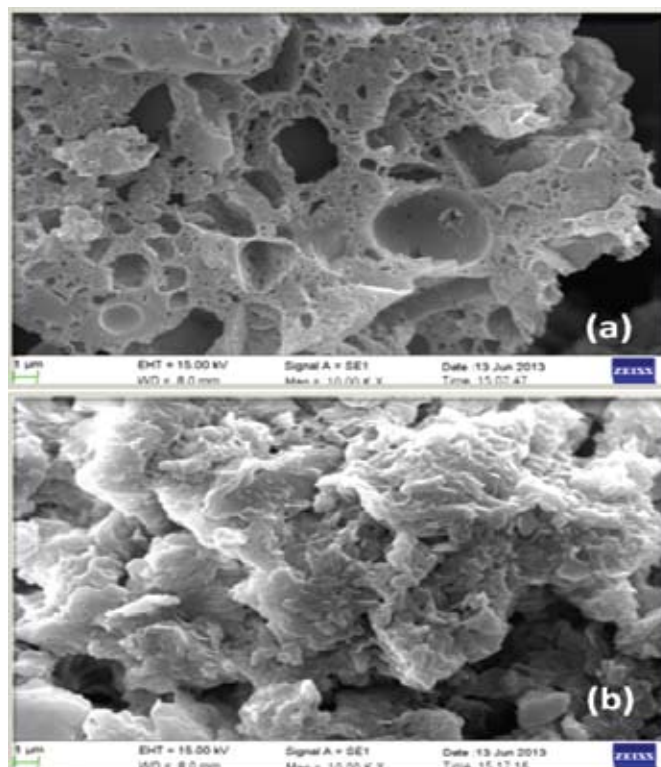


Figure 4. SEM images of CMCTS intercalated MMT (a) Before adsorption (b) After adsorption.

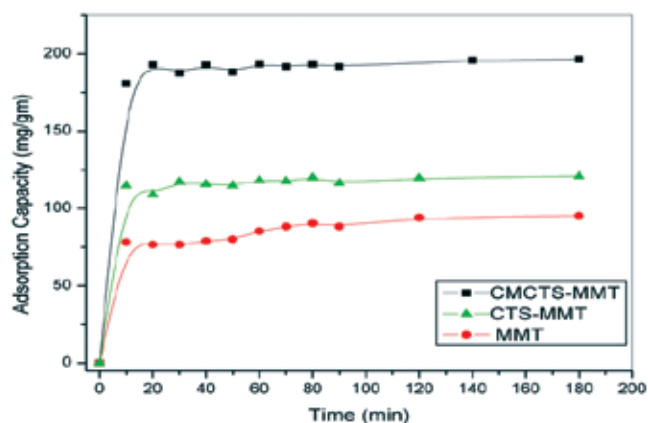
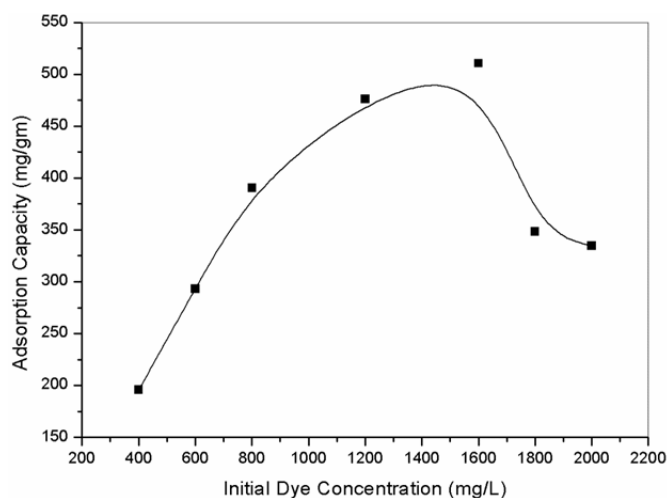


Figure 5. Effect of the adsorption time on adsorption capacity of MMT, CTS-MMT, CMCTS-MMT for CV. Adsorption experiments-Dye concentration-  $400 \text{ mg/L}$  sample dose:  $0.05 \text{ g/25 mL}$ ; pH: 8.0; temperature:  $30^\circ \text{C}$ .

of CMCTS-MMT is much higher than that of MMT and CTS-MMT. Pure MMT clays contain only negative charge, which helps to adsorb cationic CV by electrostatic interaction, but the adsorption capacity of pure MMT was very low because of its fused layer structure. On the other hand, the adsorption capacity of MMT increased after interaction of CTS with MMT. CTS consists of primary amino ( $-\text{NH}_2$ ) and hydroxyl ( $-\text{OH}$ ) groups for the adsorption of cationic CV and also increased the spacing between the layers of MMT clay. But, CMCTS-MMT showed much higher adsorption capacity compared to CTS and MMT. Carboxymethylation of chitosan introduces new active anionic carboxylic acid group ( $-\text{COO}$ ), which enhanced the adsorption capacity of CMCTS-MMT compared to other adsorbent.

### 3.5 Effect of the Initial Dye Concentration

Initial dye concentration has an important role on the adsorption capacity. In this study, the initial concentrations of dye solution were varied within the range of 400-2000 mg/L (Fig. 6). It was observed that the adsorption capacity of the sample increased from 195.84 mg/g to 510.696 mg/g with an increase in dye concentration from 400 mg/L to 1600 mg/L and reached the maximum value. With the further increase in concentration, the adsorption capacity of the CMCTS-MMT decreased gradually. The initial concentration provides an important driving force to overcome all mass transfer resistances of the CV between the aqueous and solid phases. Hence, a higher initial concentration of dye will enhance the adsorption process but after attaining maximum adsorption capacity it reaches a plateau. It indicates the saturation of active sites of the adsorbents, hence the adsorption capacity decreases further. The equilibrium conditions were reached earlier in case of low initial dye concentration than the higher initial dye concentration.



**Figure 6.** Effect of the initial dye concentration on adsorption capacity of CMCTS-MMT for CV. Adsorption experiments- sample dose: 0.05 g/25 mL; pH: 8.0; temperature: 30 °C.

### 3.6 Effect of pH

The pH of the aqueous solution plays an important role for dye separation as it affects the surface charge of the adsorbent as well as the degree of ionization of the dye molecule<sup>29</sup>. So, the adsorption experiments are carried out at different pH values between 2 and 10 to evaluate the effect of pH of the dye solution on the adsorption capacity of CMCTS-MMT. It is observed that the adsorption capacity of sample increases smoothly from 253.09 mg/g to 380.15 mg/g, when the value of pH is increased from 2 to 6 (Fig. 7). In the pH range from 6 to 8, a sharp increase in the adsorption capacity (from 380.15 mg/g to 510.696 mg/g) of CMCTS-MMT is observed. A further increase in dye adsorption between pH 8.0 and 10 is not significant. Hence, the optimum pH for dye adsorption by CMCTS-MMT is found to be 8.0. As the pH increases, the charge density of the dye solution decreases leading to the higher electronic attraction between the positively charged dye

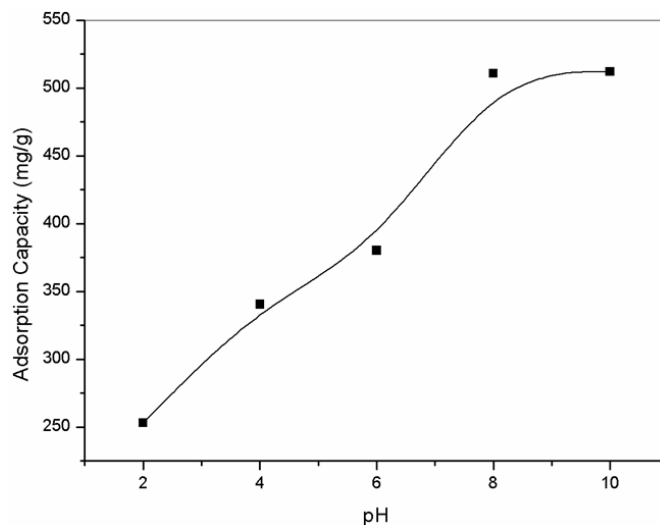


**Figure 7.** Effect of pH on adsorption capacity of CMCTS-MMT for CV. Adsorption experiments- sample dose: 0.05 g/25 mL; initial dye concentration:1600 mg/L; temperature: 30 °C.

molecule and the negatively charged surface of the adsorbent<sup>30</sup>. At lower pH of the solution, more protons are available. Hence the electrostatic repulsion between CV and positively charged adsorption sites increases, leading to a decrease in the adsorption of the cationic dyes.

### 3.7 Effect of Temperature

The effect of temperature on adsorption capacity of CMCTS-MMT was investigated at different temperatures such as 25 °C, 30 °C, 40 °C, 50 °C and 60 °C at pH 8.0 (Fig. 8). It is observed that the adsorption capacity of CMCTS-MMT for CV increased from 402.82 mg/g to 610.84 mg/g with an increase in temperature from 25 °C to 50 °C. This result suggests that the adsorption of CV on CMCTS-MMT is endothermic in nature. The increase in adsorption capacity was due to the swelling

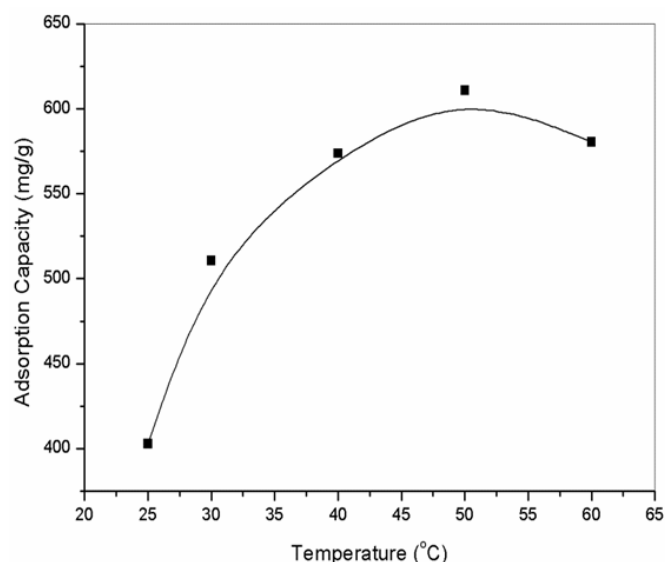


**Figure 8.** Effect of temperature on adsorption capacity of CMCTS-MMT for CV. Adsorption experiments- sample dose: 0.05 g/25 mL; initial dye concentration:1600 mg/L; pH:8.

of CMCTS-MMT with increasing temperature, facilitating the penetration of dye molecules into the internal structure of CMCTS-MMT<sup>33</sup>. This phenomenon also leads to an increment in the availability of active surface sites, increased porosity and total pore volume of the adsorbent. But, the adsorption capacity decreased to 580.46 mg/g with increasing the temperature from 50 °C to 60 °C. As the vibration of the dye molecules increase with the rise in temperature, it may be responsible for the detachment of dye molecules from the CMCTS-MMT.

### 3.8 Effect of Weight Ratio (MMT:CMCTS)

#### Variation

The effect of weight ratio of MMT:CMCTS on adsorption capacity of CMCTS intercalated MMT was investigated by varying the composition of the sample such as, MMT:CMCTS ratio of 1:1, 2:1, 4:1, 6:1, 8:1 at 30°C and at pH of 8.0. Fig. 9. reveals that the adsorption capacity of CMCTS-MMT for CV is increased periodically from 299.3 mg/g to 510.696 mg/g with the increase in the weight ratio of MMT:CMCTS from 1:1 to 4:1. But, there was a sudden decrease in adsorption capacity of CMCTS-MMT from 510.696 mg/g to 230.6 mg/g with the further increase in amount of MMT.

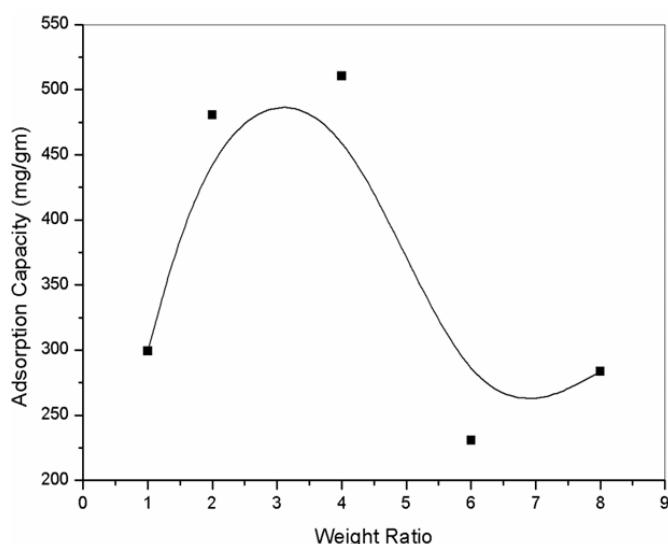


**Figure 9.** Effect of weight ratio (MMT:CMC) variation on adsorption capacity of CMCTS-MMT for CV. Adsorption experiments- sample dose: 0.05 g/25 mL; initial dye concentration:1600mg/L; pH:8; temperature: 30 °C.

### 3.9 Kinetics and Equilibrium of Adsorption

The effect of adsorption time on adsorption capabilities of CMCTS-MMT was investigated and the results are shown in Fig. 10. It was observed that the adsorption capacity of CMCTS-MMT sharply increased within 80 minutes, after that it gradually decreased. Under our experimental conditions, the equilibrium time for adsorption of CV on CMCTS-MMT is 180 min.

In order to investigate the adsorption process of CV on the adsorbent, two simplified kinetic models including pseudo-first-order and pseudo-second-order kinetic model were used for analyses.

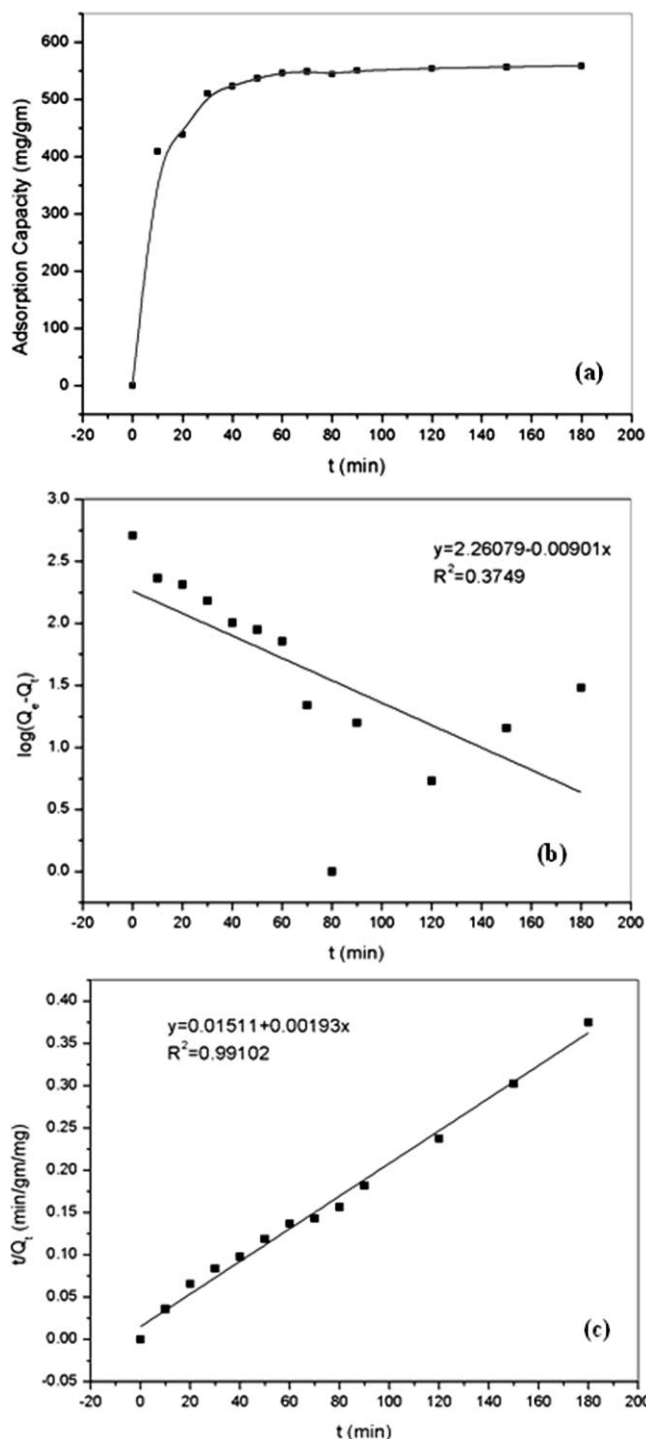


**Figure 10.** (a) Adsorption of crystal violet by CMCTS intercalated MMT as the function of time. sample dose: 0.05 g/25 mL; initial dye concentration:1600 mg/L; pH:8; temperature:30°C. (b) Linearized pseudo-first-order plot (c) Linearized pseudo-second-order plot for the adsorption of CV by CMCT-MMT.

A simple kinetic model that describes the process of adsorption is the pseudo-first-order equation. It was suggested by Lagergren<sup>34</sup> for the adsorption of solid/liquid systems and it is generally expressed as follows.

$$\frac{dQ_e}{dt} = k_1(Q_e - Q_t) \quad (2)$$

After integration with the initial condition  $Q_t=0$  at  $t=0$ , the following equation is obtained.

$$\log(Q_e - Q_t) = \log Q_e - \frac{k_1 t}{2.303} \quad (3)$$

where  $k_1$  is the pseudo-first-order rate constant ( $\text{min}^{-1}$ ),  $Q_e$  and  $Q_t$  are the amounts of dye adsorbed ( $\text{mg/g}$ ) at equilibrium and at time  $t$  ( $\text{min}$ ).

The pseudo-second order rate equation is given as

$$\frac{t}{Q_t} = \frac{1}{k_2 Q_e^2} + \frac{t}{Q_e} \quad (4)$$

where  $k_2$  is the pseudo-second order rate constant ( $\text{g mg}^{-1} \text{min}^{-1}$ ),  $Q_e$  and  $Q_t$  are the amounts of the dye adsorbed ( $\text{mg/g}$ ) at equilibrium and at a time  $t$  ( $\text{min}$ ) respectively.

The linear plots of  $\log(Q_e - Q_t)$  versus  $t$  for pseudo-first-order model (Fig. 10 (a)) and that of  $(t/Q_t)$  versus  $t$  for pseudo-second-order model (Fig. 10 (b)) are drawn. The calculated  $Q_e$ , the rate constants and the correlation coefficients for two kinetic models are shown in Table 1. The higher value of correlation coefficient (0.99102) and very close  $Q_e$  value indicate that these data are well fit for pseudo-second order.

**Table 1. Theoretically determined constants of the pseudo-first order and pseudo second-order reaction kinetics based on the sorption of crystal violet. Adsorption experiments- sample dose: 0.05 g/25 mL; initial dye concentration:1600 mg/L; pH:8.0; temperature: 30 °C**

Experimental Q (mg/g)	Pseudo-first-order constants			Pseudo-second-order constants		
	$Q_e$ (mg/g)	$K_1$ ( $\text{min}^{-1}$ )	$r^2$	$Q_e$ (mg/g)	$K_2$ ( $\times 10^{-4}$ ) ( $\text{g mg}^{-1} \text{min}^{-1}$ )	$r^2$
510.696	181.97	0.021	0.3749	518.135	2.465	0.99102

### 3.10 Adsorption Isotherm Modelling

Adsorption isotherms are mathematical models that explain the interaction of the adsorbate species with adsorbent surface. In this study, equilibrium data were analyzed using the Langmuir, Freundlich and Redlich-Peterson isotherm expressions.

#### 3.10.1 Langmuir Isotherm Model

The Langmuir isotherm model estimates the maximum adsorption capacity corresponding to complete monolayer coverage on the sample surface. The expression of Langmuir adsorption isotherm was given by Eqn (5).

$$Q_e = \frac{K_L C_e}{1 + a_L C_e} \quad (5)$$

The linear form of the above equation can be represented as follows

$$\frac{C_e}{Q_e} = \frac{1}{K_L} + \frac{a_L}{K_L} C_e \quad (6)$$

where  $C_e$  is the equilibrium dye concentration ( $\text{mg L}^{-1}$ ),  $Q_e$  is the equilibrium amount of dye adsorbed per unit weight of adsorbent ( $\text{mg g}^{-1}$ ) and  $K_L$  and  $a_L$  are Langmuir constants.

A linear plot of  $C_e/Q_e$  versus  $C_e$  for the Langmuir model of adsorption of CV on CMCTS-MMT was shown in Fig. 10 (a) and the corresponding parameters are listed in the Table 2. The favourability and feasibility of adsorption can be determined by

the dimensionless separation factor ( $R_L$ ) in the analysis of data by Langmuir isotherm which can be presented as below<sup>35</sup>.

$$R_L = \frac{1}{1 + a_L C_0} \quad (7)$$

The isotherm may be unfavourable when  $R_L > 1$ , linear for  $R_L = 1$  and favourable for  $0 < R_L < 1$  or reversible for  $R_L = 0$ . In the present study the value of  $R_L$  in all cases lies between 0 and 1 indicating that the adsorption of CV onto CMCTS-MMT is highly favourable (Fig. 11 b).

#### 3.10.2 Freundlich Isotherm Model

The Freundlich model is applicable to heterogenous systems and it involves the formation of multilayer. The Freundlich adsorption isotherm is given by the following equation.

$$Q_e = K_F C_e^{\frac{1}{n}} \quad (8)$$

The equation can be written in its linearized form:

$$\log Q_e = \log K_F + \frac{1}{n} \log C_e \quad (9)$$

**Table 2. Parameters of adsorption isotherms of crystal violet on CMCTS intercalated MMT**

Langmuir isotherm model				
$Q_{\text{max}}$ ( $\text{mg g}^{-1}$ )	$K_L$ ( $\text{Lg}^{-1}$ )	$a_L$ ( $\text{Lmg}^{-1}$ )	$r^2$	$\chi^2$
462.963	100.2	0.2164	0.9837	192.168
Freundlich isotherm model				
$K_F$ ( $\text{Lg}^{-1}$ )	$n$	$r^2$	$\chi^2$	
159.184	5.962	0.70139	206.025	
Redlich-Peterson isotherm model				
$K_R$ ( $\text{L/g}$ )	$a_R$ ( $\text{L/mmol}$ ) <sup><math>\beta</math></sup>	$\beta$	$r^2$	
13.41	0.00806	1.18	0.98672	

where,  $K_F$  and  $n$  are Freundlich constants representing adsorption capacity and adsorption intensity, respectively. These constants can be determined from the slope and intercept of linear plot of  $Q_e$  versus  $C_e$  (Fig. 11 (c)) and the values are given in Table 2. The value of  $n > 1$  in this study indicates that the process is favourable<sup>36</sup>.

Comparison of the correlation coefficient ( $r^2$ ) values from Table 2 reveals that Langmuir adsorption model yields a better fit to the experimental adsorption data than the Freundlich adsorption isotherm.

Furthermore to prevent any error in results obtained from the linearization of models, the chi-square error function was

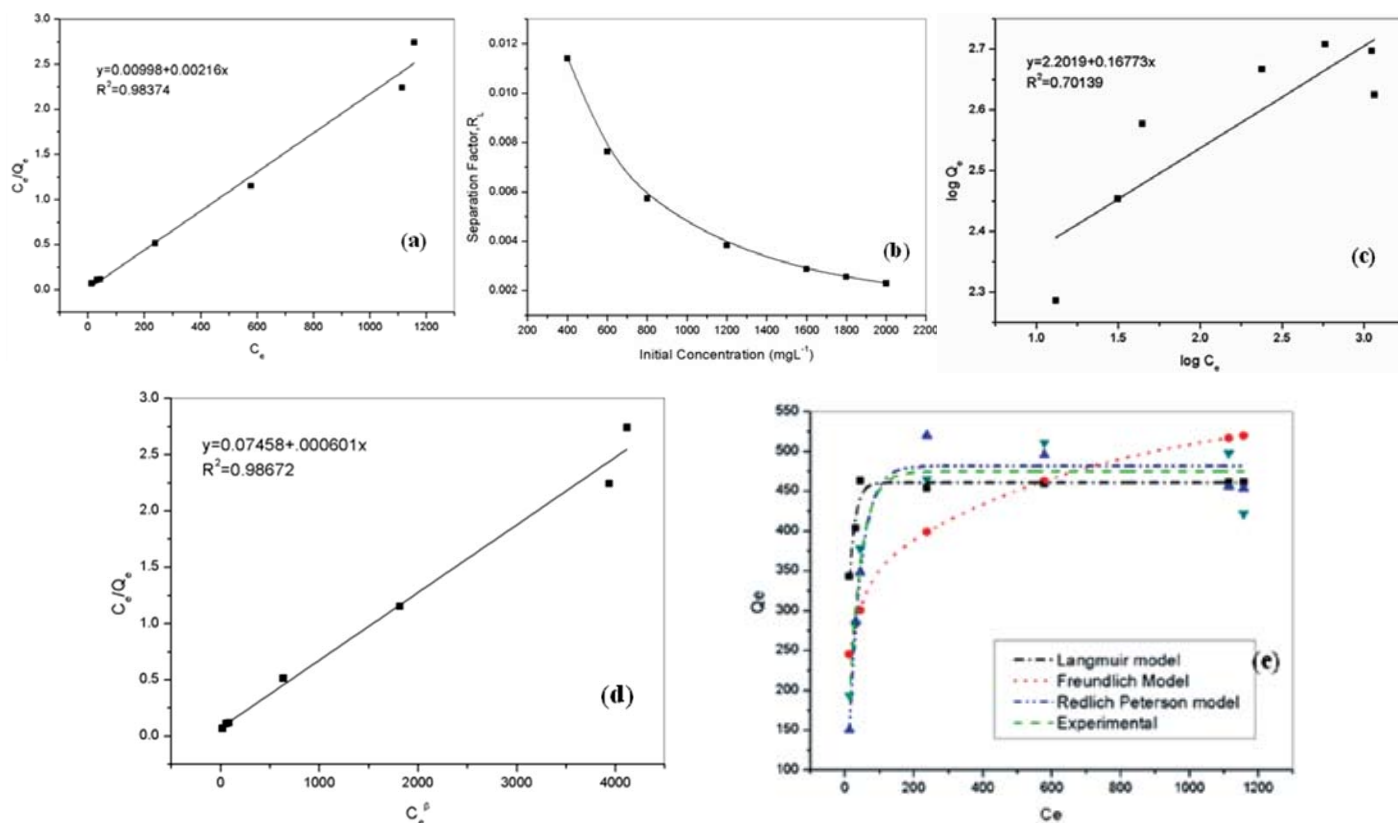


**Figure 11.** For the adsorption of CV by CMCTS-MMT: (a) The linearized Langmuir adsorption isotherms (b) Plot of separation factor versus initial dye concentration. (c) Linearized Freundlich adsorption isotherms (d) Redlich-Peterson adsorption isotherms (e) Adsorption isotherms of CV on CMCTS intercalated MMT.

calculated. Chi-square is the sum of the squares of differences between the experimental data and data predicted by the models, with each squared difference divided by the corresponding data obtained by calculating from models.

$$x^2 = \sum \left[ \frac{(Q_e - Q_m)^2}{Q_m} \right] \quad (10)$$

Table 2 indicates that the Langmuir isotherm model provides a better fit to the experimental data as  $\chi^2$  values of Freundlich model are relatively large making it unfit for the given experimental data. These results are analogous to those obtained from the linear expressions of the models.

#### 3.10.4 Redlich-Peterson Isotherm Model

Redlich-Peterson model is used as a compromise between Langmuir and Freundlich models, which can be written as<sup>37</sup>

$$Q_e = \frac{K_R C_e}{1 + a_R C_e^\beta} \quad (11)$$

where  $Q_e$  is the amount of dye adsorbed per unit mass of adsorbent at equilibrium and  $C_e$  is the equilibrium dye concentration.  $K_R$  (L/g),  $a_R$  (L/mmol) and  $\beta$  are Redlich-Peterson constants.

The above equation can be expressed in the linear form as follows

$$\frac{C_e}{Q_e} = \frac{1}{K_R} + \frac{a_R}{K_R} C_e^\beta \quad (12)$$

The Redlich-Peterson isotherm constants can be predicted from the plot between  $C_e/Q_e$  versus  $C_e^\beta$ . However, this is not possible as the linearized form of Redlich-Peterson isotherm equation contains three unknown parameters  $a_R$ ,  $K_R$  and  $\beta$ . So, a minimization method is implemented to maximize the coefficient of determination,  $r^2$  between the theoretical data for  $Q_e$  predicted from the linearized form of Redlich-Peterson isotherm equation and the experimental data.

The Redlich-Peterson isotherm plot for the adsorption of CV on CMCTS-MMT are presented in Fig. 11(d) and the isotherm parameters is given in Table 2. The higher value of  $r^2$  such as 0.9876 for the Redlich-Peterson shows that the experimental equilibrium data was found to follow Redlich-Peterson isotherm equation. This was expected because a degree of heterogeneity ( $\beta$ ) is included and this equation can be used successfully at high solute concentrations<sup>38</sup>. Langmuir is a special case of Redlich-Peterson isotherm when constant  $\beta$  is unity.

To further analyze the suitability of these three models (Langmuir, Freundlich and Redlich-Peterson), their fitness to the experimental data were investigated. In the Fig. 11(d) the different adsorption isotherms are presented in comparison with the experimental data. Hence, we can conclude Redlich-Peterson isotherm model is a better fit to the experimental equilibrium adsorption data than Langmuir and Freundlich isotherm models.

### 3.11 Desorption Study

Foreconomic feasibility of adsorbent for water purification, it is necessary to regenerate the used adsorbent. The desorption percentage of CV from CMCTS-MMT at different time intervals are presented in Fig. 12. To study the regeneration of the sample, two cycles of adsorption/desorption were carried out. It is found from the study that desorption process was reasonably fast and the equilibrium was almost reached within 70 min and the extent of desorption (%) is quite high. But, the extent of desorption (%) decreased with an increase in cycle number<sup>25,39</sup>.

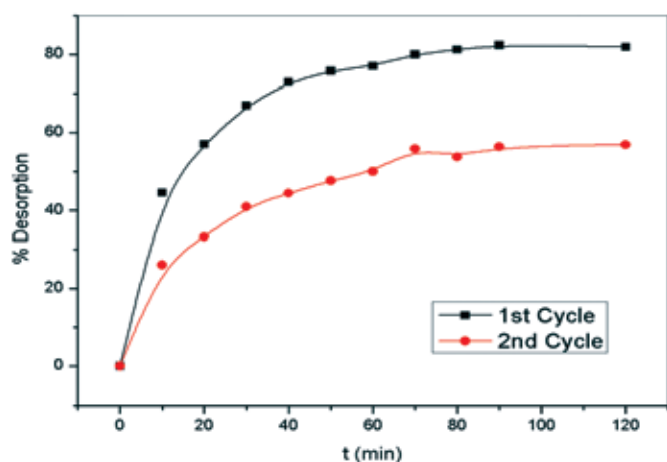


Figure 12. Desorption study of adsorbed CMCTS-MMT in 0.2 M HCl solution at different time interval.

### 3.12 Proposed Adsorption Mechanism

Figure 13 represents the FT-IR spectra of CMCTS-MMT before and after adsorption of CV dye. It is observed that there was significant change in the absorption intensity at wave numbers  $3444\text{ cm}^{-1}$  (-OH stretching vibration). Two new absorption peaks appeared at  $1588\text{ cm}^{-1}$  and at  $1368\text{ cm}^{-1}$  on adsorption of CV dye molecule onto CMCTS-MMT. This implies that the adsorption processes are physical in nature through the interaction between CV and CMCTS-MMT and may not involve a chemical interaction. The proposed mechanism of CV adsorption on CMCTS-MMT is shown in Fig. 14.

## 4. CONCLUSIONS

In this work, the potential of CMCTS intercalated MMT as an effective and low-cost adsorbent for the removal of cationic dye such as CV from the aqueous solution was investigated. Experimental results revealed that the adsorption capacity of CMCTS-MMT increases immensely than that of CMCTS and MMT individually. The effects of various parameters such as pH, temperature, initial dye concentration, composition variation on adsorption were studied. The adsorption process was fast initially, attained equilibrium within a few hours and followed the pseudo-second order kinetic model. The equilibrium data were examined by three well known adsorption isotherm models, Langmuir, Freundlich and Redlich-Peterson models, out of which Redlich-Peterson adsorption model was found to have the highest value of coefficient of determination and hence the best fit. The treated CMCTS-MMT was found

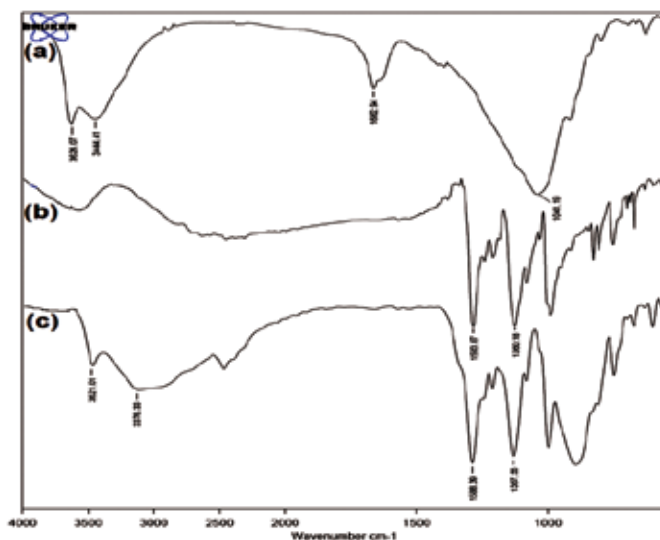


Figure 13. FTIR spectra of CMCTS intercalated MMT (a) before adsorption (b) after adsorption and (c) crystal violet dye.

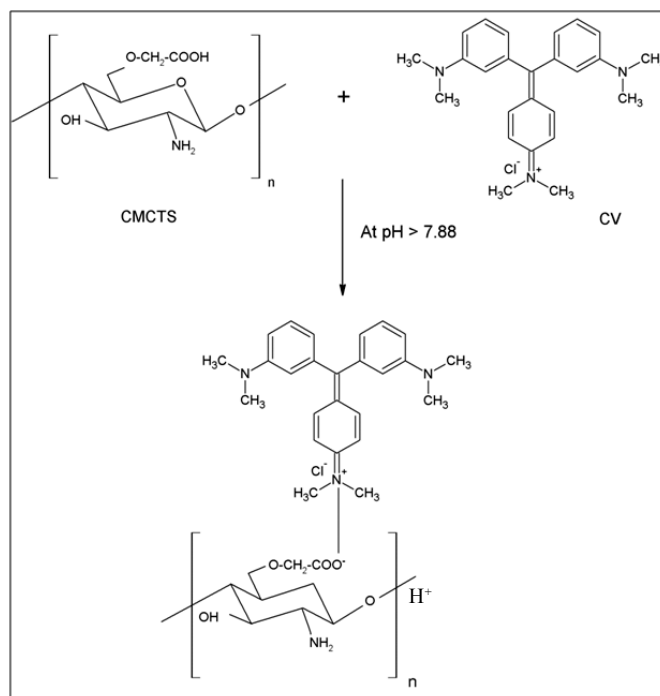


Figure 14. The proposed mechanism of CV adsorption on CMCTS intercalated MMT.

to be recyclable. Hence, we may conclude that the CMCTS intercalated MMT is a promising alternative to high cost commercial activated carbon for the removal of basic dyes from water and waste water.

## REFERENCES

1. Banat, I.M.; Nigam, P.; Singh, D. & Marchant, R. Microbial decolorization of textile dye-containing effluents: A review. *Bioresour. Technol.*, 1996, 58, 217–227.
2. Robinson, T.; McMullan, G.; Marchant, R. & Nigam, P. Remediation of dyes in textiles effluent: A critical

- review on current treatment technologies with a proposed alternative. *Bioresour. Technol.*, 2001, **77**, 247-255.
3. Auta, M. & Hameed, B.H. Preparation of waste tea activated carbon using potassium acetate as an activating agent for adsorption of Acid Blue 25 dye. *Chem. Eng. J.*, 2011, **171**, 502-509.
  4. Moghaddam, S.S.; Moghaddam, M.R. & Arami, M. Coagulation/flocculation process for dye removal using sludge from water treatment plant: Optimization through response surface methodology. *J. Hazard. Mater.*, 2010, **175**, 651-657.
  5. Sundararaman, T.R.; Ramamurthi, V. & Partha, N. Decolorization and COD Removal of Reactive Yellow 16 by Fenton Oxidation and Comparison of Dye Removal with Photo Fenton and Sono Fenton Process. *Mod. Appl. Sci.*, 2009, **3**, 15-22.
  6. Jirankova, H.; Mrazek, J.; Dolecek, P. & Cakl, J. Organic dye removal by combined adsorption-membrane separation process. *Desalination Water Treat.*, 2010, **20**, 96-101.
  7. Eyvaz, M.; Kirlaroglu, M.; Aktas, T.S. & Yuksel, E. The effects of alternating current electrocoagulation on dye removal from aqueous solutions. *Chem. Eng. J.*, 2009, **153**, 16-22.
  8. Sudarjanto, G.; Keller-Lehmann, B.; Keller, J. Optimization of integrated chemical-biological degradation of a reactive azo dye using response surface methodology. *J. Hazard. Mater.*, 2006, **138**, 160-168.
  9. Garcia-Montano, J.; Perez-Estrada, L.; Oller, I.; Maldonado, M.I.; Torrades, F. & Peral, J. Pilot plant scale reactive dyes degradation by solar photo-Fenton and biological processes. *J. Photochem. Photobiol. A. Chem.*, 2008, **195**, 205-214.
  10. Li, W.H.; Yue, Q.Y.; Gao, B.Y.; Ma, Z.H.; Li, Y.J. & Zhao, H.X. Preparation and utilization of sludge-based activated carbon for the adsorption of dyes from aqueous solutions. *Chem. Eng. J.*, 2011, **171**, 320-327.
  11. Crini, G. Non-conventional low-cost adsorbents for dye removal: A review. *Bioresour. Technol.*, 2006, **97**, 1061-1085.
  12. Babel, S. & Kurniawan, T.A. Low-cost adsorbents for heavy metals uptake from contaminated water: A review. *J. Hazard. Mater.*, 2003, **97**, 219-243.
  13. Arami, M.; Limaee, N.Y.; Mahmoodi, N.M. & Tabrizi, N.S. Removal of dyes from colored textile wastewater by orange peel adsorbent: equilibrium and kinetic studies. *J. Colloids. Interface. Sci.*, 2005, **288**, 371-376.
  14. Santos, S.C.R.; Vilar, V.J.P. & Boaventura, R.A.R. Waste metal hydroxide sludge as adsorbent for a reactive dye. *J. Hazard. Mater.*, 2008, **153**, 999-1008.
  15. Hameed, B.H. & El-Khaiary, M.I. Sorption kinetics and isotherm studies of a cationic dye using agricultural waste: broad bean peels. *J. Hazard. Mater.*, 2008, **154**, 639-648.
  16. Han, R.; Ding, D.; Xu, Y.; Zou, W.; Wang, Y.; Li, Y. & Zou, L. Use of rice husk for the adsorption of congo red from aqueous solution in column mod. *Bioresour. Technol.*, 2008, **99**, 2938-2946.
  17. Ofomaja, A.E. & Ho, Y.S. Equilibrium sorption of anionic dye from aqueous solution by palm kernel fibre as sorbent. *Dyes. Pigm.* 2007, **74**, 60-66.
  18. Eren, Z. & Nuran, F. Equilibrium and kinetic mechanism for Reactive Black sorption onto high lime soma fly ash. *J. Hazard. Mater.*, 2007, **143**, 226-232.
  19. Hameed, B.H.; Krishni, R.R. & Sata, S.A. A novel agricultural waste adsorbent for the removal of cationic dye from aqueous solutions. *J. Hazard. Mater.*, 2009, **162** 305-311.
  20. Tor, A. & Cengeloglu, Y. Removal of congo red from aqueous solution by adsorption onto acid activated red mud. *J. Hazard. Mater.*, 2006, **138**, 409-415.
  21. Ozdemir, O.; Armagan, B.; Turan, M. & Celik, M.S. Comparison of the adsorption characteristics of azo-reactive dyes on mesoporous minerals. *Dyes. Pigm.*, 2004, **62**, 49-60.
  22. Kumar, M.N.V. Ravi; Muzzarelli, R.A.A.; Muzzarelli, C.; Sashiwa, H. & Domb, A.J. Chitosan chemistry and pharmaceutical perspectives. *Chemical Reviews*, 2004, **104**, 6017-6084.
  23. Mukherjee, G.S. Calorimetric characterization of polyvinyl alcohol based membrane materials. *J. Thermal Analysis and Calorimetry*, 2009, **96**(1), 21-25
  24. Mukherjee, G.S.; Shukla, N.; Singh, R.K. & Mathur, G.N. Studies on the properties of Carboxymethylated Polyvinyl Alcohol. *J. Scientific Industrial Res.*, 2004, **63**, 596-602
  25. Sarkar, K.; Debnath, M. & Kundu, P.P. Recyclable Crosslinked O-Carboxymethyl Chitosan for Removal of Cationic Dye from Aqueous Solutions. *Hydrol. Current. Res.* 2012, **3**, 138.
  26. Wang, S.F.; Shen, L.; Tong, Y.J.; Chen, L.; Phang, I.Y.; Lim, P.Q. & Liu, T.X. Biopolymer chitosan/montmorillonite nanocomposites: Preparation and characterization. *Polym. Degrad. Stab.*, 2005, **90**, 123.
  27. Margarita, D. Biopolymer-clay nanocomposites based on chitosan intercalated in montmorillonite. *Chem. Mater.*, 2003, **15**, 3774.
  28. Adak, A.; Bandyopadhyay, M. & Pal, A. Removal of crystal violet dye from wastewater by surfactant-modified alumina. *Sep. Purif. Technol.* 2005, **44**, 139-144.
  29. hen, X.G. & Park, CH.J. Chemical characteristics of O-carboxymethyl chitosans related to the preparation conditions. *Carbohydr. Polym.*, 2003, **53**, 355-359.
  30. Zhang, J.; Wang, L. & Wang, A. Preparation and properties of chitosan-g-poly(acrylic acid)/Montmorillonite super absorbent nanocomposite via *in-situ* intercalative polymerization. *Ind. Eng. Chem. Res.*, 2007, **46**, 2497-2502.
  31. Ramakrishnan, M. & Nagarajan, S. Utilization of waste biomass for the removal of basic dye from water. *World. Appl. Sci. J.*, 2009, **5**, 114-121.
  32. Monash, P. & Pugazhenthii, G. Adsorption of crystal violet dye from aqueous solution using mesoporous materials synthesized at room temperature. *Adsorption*. 2009, **15**, 390-405.
  33. Bhattacharyya, K.G. & Sarma, A. Adsorption characteristics of the dye, brilliant green, on *Neem* leaf

- powder. *Dyes. Pigm.*, 2003, **57**, 211-222.
34. Lagergren, S. About the theory of so called adsorption of soluble substances, K. Sven. Vetenskapsakad. Hanl, 1898, **24**, 1-39.
35. Hall, K.R.; Eagleton, L.C.; Acrivos, A. & Vermeulen, T. Pore and solid diffusion kinetics in fixed bed adsorption under constant-pattern conditions. *Ind. Eng. Chem. Fundam.*, 1996, **5**, 212-223.
36. Ho, Y.S. & McKay, G. Sorption of dye from aqueous solution by peat. *Chem. Eng. J.* 1998, **70**, 115–124.
37. Redlich, O. & Peterson, D.L. A useful adsorption isotherm, *J. Phys. Chem.*, 1959, **63**, 1024.
38. Guibal, E.; Milot, C. & Tobin, M. Metal-anion sorption by chitosan beads: equilibrium and kinetic studies. *Ind. Eng. Chem. Res.*, 1998, **37**, 1454–63.
39. Kamari, A.; Wan Ngah, W.S. & Liew, L.K. Chitosan and chemically modified chitosan beads for acid dyes sorption. *J. Environ. Sci.*, 2009, **21**, 296–302.